

Phase retrieval based on coded splitting modulation

Y. YAO*, †, ‡, X. HE*, †, ‡, C. LIU*, † & JIANQIANG ZHU*, †

*Key Laboratory of High Power Laser and Physics, Shanghai Institute of Optics and Fine Mechanics, Chinese Academy of Sciences, Shanghai, China

†National Laboratory on High Power Laser and Physics, Shanghai, China

‡University of Chinese Academy of Sciences, Beijing, China

Key words. Diffractive optics, Fourier optics and signal processing, phase measurement, phase retrieval.

Summary

A new coded splitting imaging technique is proposed to reconstruct the complex amplitude of a light field iteratively using a single-shot measurement. In this technique, a specially designed coded splitting plate is adopted to diffract the illuminating beam into multiple beams of different orders and code their wavefronts independently and differently. From the diffraction pattern array recorded on the detector plane, both the modulus and phase distributions of the illuminating beam can be reconstructed iteratively using known transmission functions of different orders of the coded splitting plate. The feasibility of the proposed technique is verified both numerically and experimentally.

Introduction

Coherent diffraction imaging (CDI) method is a lensless imaging technique that can measure the phase and modulus distributions of a light field from the intensity of recorded diffraction patterns using an iterative approach. Since it does not require high-quality optics and can obtain diffraction limited spatial resolution theoretically, CDI can be adopted to observe a sample with a broad range of radiations including visible light, high-energy electron, and X-ray photons and has become an independent tool in many research fields (Fienup, 1993; Köstli and Beard, 2003; Zuo *et al.*, 2003; Roy *et al.*, 2011). The first widely accepted CDI technique is the G–S algorithm proposed by Gerchberg and Saxton (Gerchberg, 1972). Moreover, it was further developed using Fienup algorithms and an oversampling method (Fienup, 1982; Miao *et al.*, 2003) and it can retrieve complex amplitude with a single frame of diffraction pattern intensity. Although these CDI algorithms based on the G–S algorithm demonstrated significant achievements in imaging samples with short wavelengths including X-ray and electron beam, they also suffer from problems such as

low convergence speed, limited field of view, and low reliability, especially in imaging large objects with complex phase distributions (Fienup and Wackerman, 1986; Fienup, 1987). Many modified CDI algorithms have been proposed to overcome these drawbacks, and they can be generally divided into two categories. The first group, termed as multishot CDI, involves using a multiwavelength source for illumination (Bao *et al.*, 2008), scanning the diffraction field axially (Ivanov *et al.*, 1992; Allen and Oxley, 2001; Almoró *et al.*, 2006), scanning the sample transversely (Faulkner and Rodenburg, 2004; Maiden and Rodenburg, 2009), and scanning the illuminating direction (Ou *et al.*, 2013; Bian *et al.*, 2014; Dong *et al.*, 2015). Significant data redundancy in these algorithms offers several remarkable advantages over conventional CDI methods, including significant improvement in robustness to noise, no requirement for prior knowledge of the sample, faster convergence speed, and more reliable reconstruction. However, these methods require significant data acquisition time, precluding their application for imaging fast dynamics. Furthermore, since these methods rely heavily on the stability of the imaging system, both vibration and degeneration of the sample may result in failure of the experiments. Note that even tiny imprecisions in the scanning steps can degrade the reconstructed resolution. The second group, termed as single-shot CDI, can realize real-time measurement of a light field. The recently developed coherent modulation imaging method uses a random phase plate to modulate the light field, and it adopts a spatial constraint at the entrance plane which is usually the focal plane (Zhang and Rodenburg, 2010; Tao *et al.*, 2016). However, since only one frame of diffraction patterns is applied, the reconstruction is noisy when compared to that of multishot CDI algorithms. In order to obtain high-quality reconstruction with single-shot measurement, a feasible approach is to record a diffraction pattern array with a single exposure of detector to increase data redundancy, and based on this idea, two kinds of single-shot ptychography methods have been demonstrated (Pan *et al.*, 2013; Sidorenko and Cohen, 2016). In Pan *et al.* (2013), a cross-grating was adopted to diffract the illumination beam into a laser beam cluster to

Correspondence to: Cheng Liu, Shanghai Institute of Optics and Fine Mechanics, Chinese Academy of Science, No. 390, Qinghe Rd., Jiading, Shanghai 201800, China. Tel: +86-21-69918799; e-mail: cheng.liu@hotmail.co.uk

illuminate the sample to generate the diffraction pattern array. Furthermore, in Sidorenko and Cohen (2016), a pinhole array and an asymmetric 4f system were adopted to realize overlapping illumination and single-shot measurement. However, in these two methods, all the diffracted beams should be exactly the same except for the phase ramp, and the two neighbouring diffracted beams should properly overlap on the sample plane; thus, the requirements of the quality of the grating and other optics are very critical, and the experimental setups are always complex. Reconstructing a general complex-valued dynamic object reliably and rapidly from a single diffraction pattern is extremely difficult. Moreover, it would be highly beneficial to have a phase retrieval method that benefits from large data redundancy and can function with a single-shot measurement.

In this study, a coded splitting imaging technique is proposed, where the light from the sample is diffracted into several orders forming a diffraction pattern array on the detecting plane. By contrast to a common cross-grating whose diffraction beams of diffraction orders are duplicates of each other except for the phase ramps, the coded splitting plate (CSP) used in this study is specially designed to code each diffraction order separately and differently, rendering their transmission functions entirely different from each other. Thus, the information included in an illuminating beam incident on the CSP is fully coded in the recorded diffraction pattern array. With the known transmission function of the CSP, the modulus and phase distributions of the incident beam can be faithfully reconstructed iteratively. Since only one piece of additional CSP is required in comparison with conventional CDI techniques, the proposed method has a simple experimental setup. However, since multiple diffraction patterns recorded with one exposure are used to perform the reconstruction, the proposed method has high data redundancy similar to multishot CDI and accordingly has high noise resistance capability and fast convergence speed.

Principle of the coded splitting method

The principle of the coded splitting imaging method is illustrated in Figure 1(A), where the experimental setup is simple, containing only a CSP and a charge coupled device (CCD). The

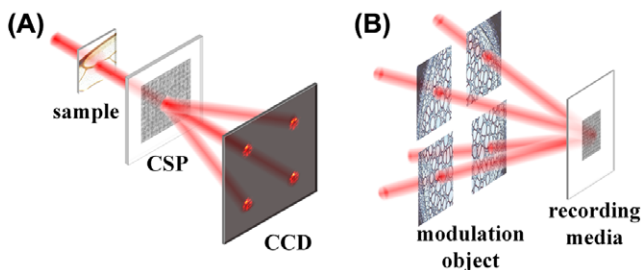


Fig. 1. (A) Scheme of coded splitting method; (B) basic idea of fabricating the CSP.

incident beam passes through the sample and subsequently incidents onto the CSP, and the generated diffraction pattern array is recorded using the CCD camera.

Design of the CSP

The key component of the proposed method is the CSP, whose transmission function can be regarded as a twisted cross-grating and can be mathematically expressed as

$$T(x_0, y_0) = \sum_{m,n} P_{mn}(x_0, y_0) \exp[j(k_m x_0 + k_n y_0)], \quad (1)$$

where (x_0, y_0) are coordinates in the CSP plane, (k_m, k_n) represents the spatial frequency of the (m, n) th order of diffraction, and $P_{mn}(x_0, y_0)$ represents the corresponding transmission. Figure 1(B) illustrates the basic idea of fabrication of the CSP, where several parallel beams illuminate a recording media (such as a holographic plate) after passing through the corresponding modulation objects to form an irregular grating by interfering with each other coherently; vice versa, under the illumination of a laser beam, this recorded irregular grating can diffract the incident beam to a beam cluster, and all the diffracted beams have wavefronts different from each other. In other words, the twisted grating in Figure 1(B) can be used as the CSP of the proposed technique.

In practice, a pure-phase CSP can be generated using the G-S algorithm (Gerchberg, 1972). Subsequently, the generated CSP can be transferred to a physical glass substrate using photo-etching or can be directly shown on a spatial light modulator (SLM). As shown in Figure 2, an iterative regime to design the CSP is carried out between the CSP plane and the diffraction plane, and begins with an initial guess of the transmission function of the CSP $T^c(x_0, y_0) = \sum_{m,n} P_{m,n}^c(x_0, y_0) \exp[j(k_m x_0 + k_n y_0)]$, where $P_{m,n}^c(x_0, y_0)$ are the initial guesses of modulators of different diffraction orders. Usually, we can use different pictures to act as the initial modulators. In the CSP plane, the transmission function of the CSP is updated with a constraint of the pure phase distribution. Subsequently, the CSP is illuminated using a plane wave $E(x_0, y_0)$, and the beams diffracted from the CSP form a diffraction pattern array $D(x, y)$, where (x, y) represents the coordinates in the diffraction plane. The diffraction pattern array is updated with a constraint that can ensure that the diffraction patterns do not overlap with each other. In the simulation and the experiments in this paper, we used a constraint that force values in regions between different diffraction patterns to be zero on the diffraction plane. And the widths of these regions are usually one-tenth of the distances between different diffraction patterns. Further, the updated diffraction array is expressed as $D(x, y)$. When the difference between the calculated and updated diffraction pattern arrays is smaller than the set threshold, the iteration is completed, and $T(x_0, y_0)$ is considered as the designed transmission function of the CSP.

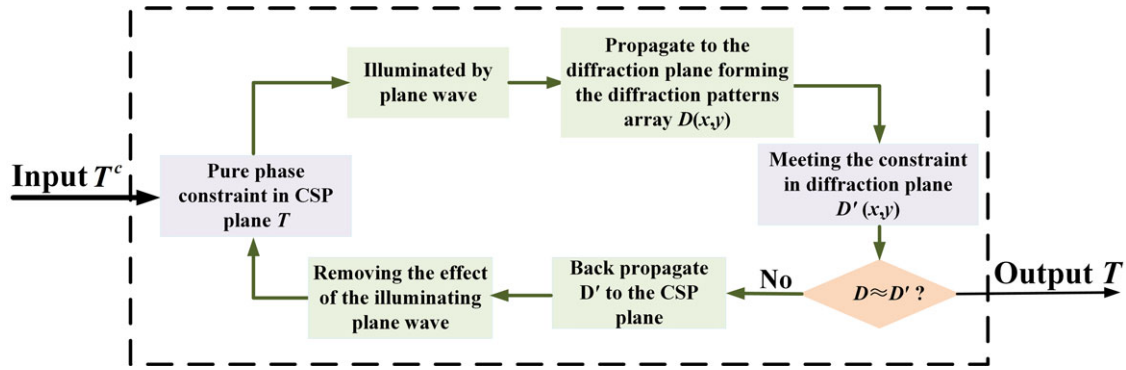


Fig. 2. Schematic of generating pure-phase CSP using the G-S algorithm.

Description of the algorithm

When the frequency bandwidth of $P_{mn}(x_0, y_0)$ is smaller than the spatial frequency gaps between the (m, n) th order and the $(m \pm 1, n \pm 1)$ th orders, each diffraction pattern formed by the corresponding diffraction orders will be clearly separated from others on the detector plane, forming a diffraction pattern array. Therefore, the intensity pattern recorded by the CCD consists of clearly distinguished $M \times N$ diffraction patterns and each of them occupies a separate region. Moreover, we can associate each region and its diffraction pattern with a specific $P_{mn}(x_0, y_0)$. Before the iterative reconstruction, each diffraction pattern should be extracted from the diffraction pattern array into separate matrixes to avoid the complexity of considering the direction of (k_m, k_n) in the iterative computation.

Considering the computational error and the display or manufacturing error of the CSP, transmission functions $P_{mn}(x_0, y_0)$ of each diffraction order need to be premeasured. With the known $P_{mn}(x_0, y_0)$, the information of the incident light beam embedded in the diffraction array can be faithfully retrieved iteratively from the recorded diffraction pattern array. After an initial guess $W(u, v)$ is provided to the exiting wave field of the sample and propagated to the CSP plane to obtain the illumination on the CSP $U(x_0, y_0) = \mathfrak{F}\{W(u, v)\}U(x_0, y_0) = I\{W(u, v)\}$, where (u, v) represents the coordinates in the sample plane, iterative reconstruction can be carried out with the following steps.

- (1) The (m, n) th order of diffraction leaving the CSP is

$$V_{mn,i}(x_0, y_0) = U_i(x_0, y_0) \cdot P_{m,n}(x_0, y_0), \quad (2)$$

where i represents the number of iterations.

- (2) Then, $V_{mn,i}(x_0, y_0)$ is propagated to the detector plane

$$\psi_{mn,i}(x, y) = F_z \{V_{mn,i}(x_0, y_0)\} = |\psi_{mn,i}| \exp(j\phi_{mn,i}), \quad (3)$$

where F_z denotes numerical wave propagation. The modulus is replaced by the square root of the diffraction intensity I_{mn} of the recorded (m, n) th order

$$\psi_{mn,i}^c(x, y) = \sqrt{I_{mn}} \exp(j\phi_{mn,i}), \quad (4)$$

where the superscript c indicates the function after updating.

- (3) The updated wave function $\psi_{mn,i}^c(x, y)$ is propagated back to the CSP plane as

$$V_{mn,i}^c(x_0, y_0) = F_{-z} \{ \psi_{mn,i}^c(x, y) \}, \quad (5)$$

where F_{-z} represents the inverse propagation progress.

- (4) The illumination on the CSP plane is updated using the Wigner filter-like formula (Faulkner and Rodenburg, 2004; Maiden and Rodenburg, 2009) as

$$U_i^c = U_i + \frac{|P_{mn}|}{|P_{mn}|_{\max}} \frac{P_{mn}^*}{[|P_{mn}|^2 + \alpha]} (V_{mn,i}^c - V_{mn,i}), \quad (6)$$

where $*$ represents the conjugate process, and α is a properly chosen constant to prevent a zero denominator in Eq. (6).

- (5) Steps (1)–(4) are repeated using another set of $P_{mn}(x_0, y_0)$ and I_{mn} until all the recorded diffraction patterns are addressed.
- (6) The accuracy of the reconstruction is verified using the following equation. If the accuracy reaches a certain value and the computation stops, the exiting wave field of the sample can be obtained by backward propagating $U^c(x_0, y_0)$ to the sample plane $W(u, v) = F_{-z} \{U^c(x_0, y_0)\}$; otherwise, return to step (1) to start another round of computation:

$$Err_i = \frac{\sum_{m,n} \sum_{x,y} |\sqrt{I_{mn}} - |\psi_{mn,i}||^2}{\sum_{m,n} \sum_{x,y} I_{mn}}. \quad (7)$$

Results and discussion

Number of diffraction patterns

The feasibility of the proposed technique was first verified using numerical simulations to determine the number of diffraction patterns required. The light field to be measured was an emitted

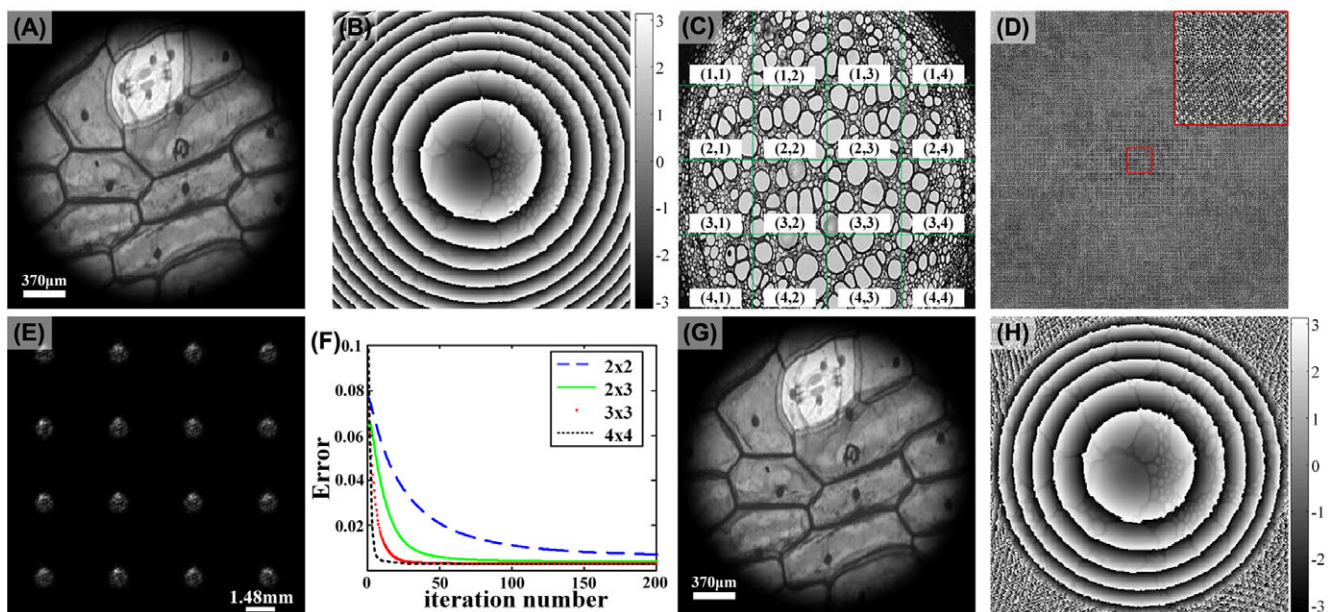


Fig. 3. Original (A) modulus and (B) phase of the light field emitted from the tested sample; (C) picture used to modulate the phase of each diffraction order; (D) phase distribution of the CSP; the upper inset is the close-up of the region in the red square; (E) recorded intensity containing array of 4×4 diffraction patterns; (F) convergence performance of coded splitting method using different number of diffraction patterns in recording intensity; reconstructed (G) modulus and (H) phase of the measured light field using 3×3 diffraction patterns.

wave from a test object illuminated by a convergent Gaussian laser beam. The modulus of the transmission function of the sample was a fractal pattern with values varying from 0.1 to 1, and the phase varied from 0 to $\pi/2$. The diameter of the incident light field was assumed to be 2.22 mm, and the size of each pixel was assumed to be $7.4 \mu\text{m}$. The amplitude and phase distribution of the emitting light field from the sample are shown in Figures 3(A) and (B), respectively. The sample was placed 20 mm before the CSP, and the distance between the detector and CSP was 194 mm. Figure 3(C) shows the picture used to modulate the phase of each diffraction order, where the 4×4 parts of the picture act as the initial modulators of 16 orders of diffraction beams. Figure 3(D) shows the generated pure-phase CSP with the aid of the G–S algorithm. Figure 3(E) shows the diffraction patterns formed on the detector plane.

First, we examined the influence of the number of diffraction patterns on the quality of the final reconstruction by computing the error of the reconstruction, which is defined in Eq. (7). The result is shown in Figure 2(F), where we can observe that, with the increasing in the number of diffraction patterns used, the convergence speed and accuracy of the final reconstruction will become remarkably better. This also supports the idea that the data redundancy can improve the reconstruction quality and convergence speed. Furthermore, when 3×3 diffraction patterns are used for reconstruction, the error of the final reconstruction can be much lower than 0.01 and both the modulus and phase of the reconstructed light field are very clear (see Figs. 3G, H for detail). Since the size of the

sensitive chip of the detector is not very large, we used 3×3 diffraction patterns in our proof-of-principle experiment.

Experimental results

Feasibility of the proposed method was verified experimentally using a He–Ne laser (NewOpto, China). The experimental setup is shown in Figure 4. An SLM (Holoeye, Germany) with 1920×1080 pixels (pixel size is $6.4 \mu\text{m}$) was used as the CSP to code the measured light field. A $\lambda/2$ wave plate was used to adjust the polarization direction of the illumination field to ensure that the SLM operates in the pure-phase mode. The parallel light beam from the spatial light filter was limited by an aperture of diameter approximately 2.5 mm and, subsequently, this beam illuminated the sample, which was a fixed biological sample of a bee wing. The CSP shown in the SLM splits the illumination into 3×3 differently modulated diffraction beams forming the diffraction patterns array on the CCD camera (Allied Vision Technologies, Germany), which has 4008×2672 pixels (pixel size is $9 \mu\text{m}$). The distance between the SLM and sample and that between the sample and CCD were 60.193 mm and 289.03 mm, respectively.

Figure 5(A) shows the recorded intensity when the sample is empty, where each diffraction pattern occupies an isolated area in the detector plane. Using the reconstruction procedure illustrated above, the illumination on the CSP plane was clearly reconstructed, and the reconstructed modulus and phase are shown in Figures 5(B) and (C), respectively. After the sample was placed into the optical path, another

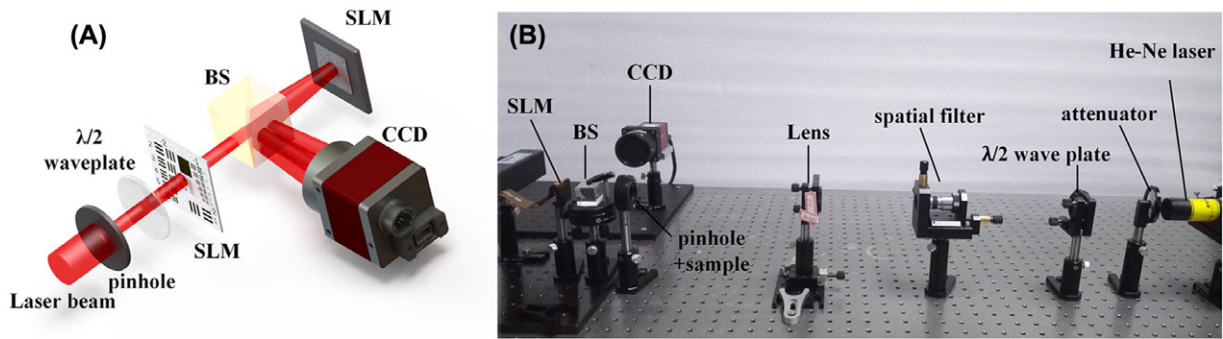


Fig. 4. (A) Simplified schema of the experimental setup; (B) photo of the experimental setup.

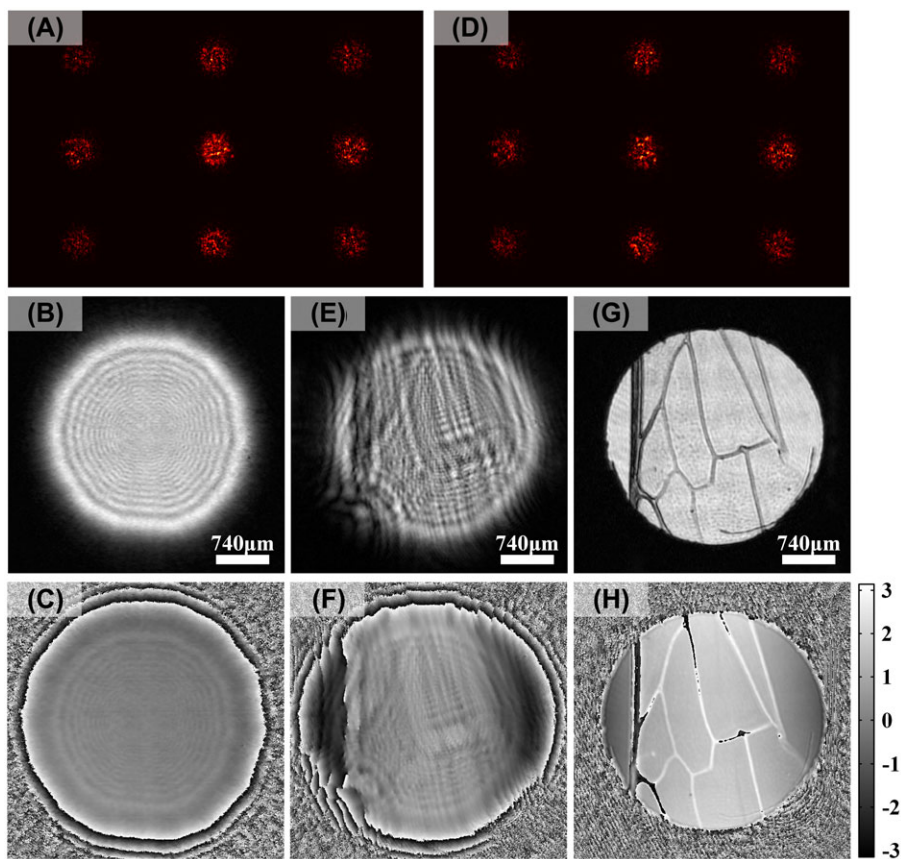


Fig. 5. (A) Recorded intensity when the sample is empty; reconstructed (B) modulus and (C) phase distribution of the incident light field on the CSP when the sample is empty; (D) recorded intensity with the biological sample; reconstructed (E) modulus and (F) phase distribution of the incident light field on the CSP with the biological sample; reconstructed (G) modulus and (H) phase of the sample.

diffraction pattern array shown in Figure 5(D) was recorded, and the modulus and phase of the light field on the CSP were reconstructed and shown in Figures 5(E) and (F), respectively. By backward propagating the reconstructed light field to the sample plane and taking out the influence of the illumination, the complex amplitude of the sample can be obtained. Figures 5(G) and (H) show the modulus and phase of the sample, respectively, wherein the skeleton structure of the bee

wing can be obviously observed. However, some fine structures of the sample cannot be clearly resolved. This is because the achievable resolution of this experiment is limited to the pixel size of the SLM, and we will discuss this problem in the next section. In addition, another reason is that when measuring some strongly scattering sample, some frequency components will inevitably enter neighbouring regions and then generate noise in the reconstruction.

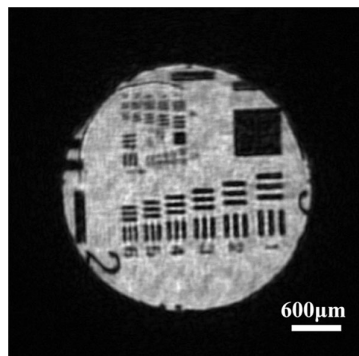


Fig. 6. Reconstructed image of the USAF 1951 target.

Resolution

In order to estimate the resolution of the coded splitting method, the maximum (the cutoff) spatial frequency ν_{\max} of the sample that can be detected by the diffraction pattern array is calculated. The coordinate transform is described as $\nu = x/\lambda L$, where ν is the spatial frequency of the sample, x is the coordinate on detector plane, and L is the distance between the sample and CCD. The width of region occupied by each diffraction pattern in the detector plane is d . So, the cutoff frequency is $\nu_{\max} = d/2\lambda L$. This indicates that the resolution is determined by the light splitting ability of the CSP, and in some spectral regions (for example, visible light), the resolution of the coded splitting method can be close to the order of wavelength by using a CSP with small grating period.

We also quantified the resolution by measuring a United State Air Force (USAF) 1951 resolution target using the experimental setup mentioned above. Further, the reconstructed image is shown in Figure 6, where we can observe that the second elements in group 4 can be distinguish, so the resolution achievable is $27.8 \mu\text{m}$ (17.95 lp mm^{-1}). The resolution of the above experiment can be calculated using the relationship $\nu_{\max} = d/2\lambda L$, where d is $(2672/3 \times 9) \mu\text{m}$, L is $(60.193 + 289.03) \text{ mm}$, and λ is $0.6328 \mu\text{m}$. Further, ν_{\max} is calculated to be $0.0181 \mu\text{m}^{-1}$, such that the theoretical resolution $\Delta x = 1/2\nu_{\max}$ is $27.55 \mu\text{m}$, which is consistent with the measured resolution. As we discussed above, the achievable resolution is determined by the beam splitting ability of the CSP. In the experiment mentioned above, the generated CSP was displayed on the SLM, so its minimum grating period needs to be at least two times larger than the pixel size of the SLM to accurately realize the beam splitting function. Higher resolution can be obtained by using a SLM with smaller period size or manufacturing CSP with smaller grating period using photoetching technique.

Summary

In summary, we proposed a single-shot phase retrieval method using a specially designed CSP to split the incident beam into

multibeam and code their wavefronts separately and differently. Each diffraction beam generated an isolated diffraction pattern in the detector plane, forming a diffraction pattern array that can be recorded simultaneously with a CCD exposure. The modulus and phase of the incident light field were faithfully reconstructed from the recorded diffraction pattern array. The proposed method utilizes the benefits of both the multishot CDI method, which has fast convergence speed and high noise immunity, and single-shot CDI method, which has a simple experimental setup and fast data acquisition. As a single-shot technique, the data acquisition time of the proposed method is determined by the exposure time of the CCD detector, which usually takes several milliseconds. So, it has many potential applications in fast imaging; for example, it is of great importance to the biomedical imaging of a dynamic sample such as fresh living cells or tissues (for example, the early stage embryo of zebra fish), and it provides a good choice to measure the wavefront of the pulse light of a high-power laser with low repetition. Furthermore, it can also be extended to the short wavelength region. Moreover, the coded splitting method can be further improved: (1) The CSP can be further optimized to enable the proposed method to be more applicable to short wavelength imaging. An amplitude plate with the same function will be significant because it has low requirements for manufacture; (2) The interacting information between different diffraction patterns, which is treated as noise and is neglected in the current algorithm, may be useful to retrieve more information and break the resolution limit imposed by the assumption of separate regions, which will be studied in detail in the future. Finally, we believe that the coded splitting method can provide new opportunities in dynamic imaging.

Funding

National Natural Science Foundation of China (No. 61675215).

References

- Allen, L.J. & Oxley, M.P. (2001) Phase retrieval from series of images obtained by defocus variation. *Optics Commun.* **199**, 65–75.
- Almoro, P., Pedrini, G. & Osten, W. (2006) Complete wavefront reconstruction using sequential intensity measurements of a volume speckle field. *Appl. Opt.* **45**, 8596–8605.
- Bao, P., Zhang, F., Pedrini, G. & Osten, W. (2008) Phase retrieval using multiple illumination wavelengths. *Opt. Lett.* **33**, 309–311.
- Bian, L., Suo, J., Situ, G., Zheng, G., Chen, F. & Dai, Q. (2014) Content adaptive illumination for Fourier ptychography. *Opt. Lett.* **39**, 6648–6651.
- Dong, S., Nanda, P., Guo, K., Liao, J. & Zheng, G. (2015) Incoherent Fourier ptychographic photography using structured light. *Photonics Res.* **3**, 19–23.
- Faulkner, H. & Rodenburg, J. (2004) Movable aperture lensless transmission microscopy: a novel phase retrieval algorithm. *Phys. Rev. Lett.* **93**, 023903.

- Fienup, J.R. (1982) Phase retrieval algorithms: a comparison. *Appl. Opt.* **21**, 2758–2769.
- Fienup, J.R. (1987) Reconstruction of a complex-valued object from the modulus of its Fourier transform using a support constraint. *J. Opt. Soc. Am. A* **4**, 118–123.
- Fienup, J.R. (1993) Phase-retrieval algorithms for a complicated optical system. *Appl. Opt.* **32**, 1737–1746.
- Fienup, J.R. & Wackerman, C.C. (1986) Phase-retrieval stagnation problems and solutions. *J. Opt. Soc. Am. A* **3**, 1897–1907.
- Gerchberg, R.W. (1972) A practical algorithm for the determination of phase from image and diffraction plane pictures. *Optik* **35**, 237–246.
- Ivanov, V.Y., Vorontsov, M.A. & Sivokon, V.P. (1992) Phase retrieval from a set of intensity measurements: theory and experiment. *J. Opt. Soc. Am. A* **9**, 1515–1524.
- Köstli, K.P. & Beard, P.C. (2003) Two-dimensional photoacoustic imaging by use of Fourier-transform image reconstruction and a detector with an anisotropic response. *Appl. Opt.* **42**, 1899–1908.
- Maiden, A. & Rodenburg, J. (2009) An improved ptychographical phase retrieval algorithm for diffractive imaging. *Ultramicroscopy* **109**, 1256–1262.
- Miao, J., Ishikawa, T., Anderson, E.H. & Hodgson, K.O. (2003) Phase retrieval of diffraction patterns from noncrystalline samples using the oversampling method. *Phys. Rev. B* **67**, 174104.
- Ou, X., Horstmeyer, R., Yang, C. & Zheng, G. (2013) Quantitative phase imaging via Fourier ptychographic microscopy. *Opt. Lett.* **38**, 4845–4848.
- Pan, X., Liu, C. & Zhu, J. (2013) Single shot ptychographical iterative engine based on multi-beam illumination. *Appl. Phys. Lett.* **103**, 171105.
- Roy, S., Parks, D., Seu, K.A., *et al.* (2011) Lensless X-ray imaging in reflection geometry. *Nat. Photonics* **5**, 243–245.
- Sidorenko, P. & Cohen, O. (2016) Single-shot ptychography. *Opt.* **3**, 9–14.
- Tao, H., Veetil, S.P., Pan, X., Liu, C. & Zhu, J. (2016) Lens-free coherent modulation imaging with collimated illumination. *Chinese Optics Lett.* **14**, 071203.
- Zhang, F. & Rodenburg, J.M. (2010) Phase retrieval based on wave-front relay and modulation. *Phys. Rev. B* **82**, 121104.
- Zuo, J.M., Vartanyants, I., Gao, M., Zhang, R. & Nagahara, L.A. (2003) Atomic resolution imaging of a carbon nanotube from diffraction intensities. *Science* **300**, 1419–1421.